

Coherent Dark State Formation of a Lead-Vacancy Spin Qubit in Diamond

Yiyang Chen,¹ Koyo Hirai,¹ Tzyy Zheng Neo,¹ Eiki Ota,¹ Takashi Taniguchi,² Masashi Miyakawa,² Shinobu Onoda,³ Toshiharu Makino,⁴ Mutsuko Hatano,¹ and Takayuki Iwasaki^{1,*}

¹*Department of Electrical and Electronic Engineering, School of Engineering, Institute of Science Tokyo, Meguro, Tokyo 152-8552, Japan*

²*International Center for Materials Nanoarchitectonics, National Institute for Materials Science, Tsukuba, Ibaraki 305-0044, Japan*

³*Takasaki Advanced Radiation Research Institute, National Institutes for Quantum Science and Technology, 1233 Watanuki, Takasaki, Gunma 370-1292, Japan*

⁴*Advanced Power Electronics Research Center, National Institute of Advanced Industrial Science and Technology, Tsukuba, Ibaraki 305-8568, Japan*

A lead-vacancy (PbV) center in diamond exhibits coherent emission above the liquid helium temperature, making it highly attractive for quantum network applications. Here, we report the magneto-optical and spin properties of PbV centers in diamond. We record a spin lifetime of 12 ms at 7.5 K under large off-axis magnetic field. Furthermore, we observe formation of the coherent dark state by coherent population trapping and estimate a spin dephasing time of 354 ns at 6.5 K. This work demonstrates the outstanding thermal robustness of the PbV spin compared to other group-IV centers above 4 K.

The realization of quantum networks is fundamental to the advancement of quantum information processing[1]. Beyond establishing a platform for unconditionally secure quantum communication, quantum networks enhance the security of quantum computation and push the sensitivity of quantum metrology toward its physical limits[2]. As such, the development of quantum networks has emerged as a main focus of quantum information processing. Quantum emitters in quantum network nodes including quantum repeaters are essential to achieve scalable quantum networks. Defects in diamond have emerged as promising candidates for the quantum emitters, leveraging their long-lived quantum memory[3–7] and reliable spin-photon interfaces[8, 9]. The multi-node quantum networks based on nitrogen-vacancy (NV) centers have been demonstrated[10]. However, the low concentration into the zero-phonon line (ZPL) and spectral diffusion significantly limit its scalability. To address these challenges, the group-IV defects including silicon-vacancy[11], germanium-vacancy[12], tin-vacancy[13], and lead-vacancy[14] (SiV, GeV, SnV, and PbV, respectively) have been proposed. These defects exhibit a ZPL concentration around an order of magnitude higher than that of NV centers. Furthermore, owing to their intrinsic inversion symmetry, spectral diffusion is significantly suppressed. These favorable properties have already enabled milestones such as metropolitan-scale quantum networks[15], blind quantum computing[16], and enhanced quantum interferometry[17] using SiV centers.

However, the group-IV centers are susceptible to phonon-mediated decoherence in the ground state. Consequently, the SiV and GeV centers require millikelvin temperatures to obtain a long spin coherence time by suppressing the phonon interaction[4, 5]. The SnV cen-

ter typically necessitates temperatures around 2 K[6] below the liquid helium temperature. In contrast, the PbV center stands out with the largest ground state zero field splitting (ZFS) of ~ 3900 GHz[14] among the group-IV centers, which significantly suppresses the electron-phonon interaction. This makes the PbV center a unique candidate predicted to have a long spin coherence time above 4 K. The suppression of the phonon interaction in the PbV center has been observed as the transform-limited linewidth even above 10 K[18]. However, the spin properties of the PbV qubit have remained elusive. In this work, we report the magneto-optical and spin properties of the PbV centers. We demonstrate all-optical spin initialization and readout, a long spin relaxation time (T_1), and the coherent dark state formation leading to the estimation of a spin dephasing time (T_2^*). Our results verify the predicted excellent thermal robustness of PbV over 4 K, highlighting its potential for scalable quantum networks.

Upon Pb ion implantation into the diamond lattice, followed by high-temperature annealing under high-pressure[14, 19], Pb atoms combine with vacancies in diamond to form a split-vacancy structure oriented along the $\langle 111 \rangle$ crystallographic axis. This specific configuration constitutes the PbV color centers in diamond with localized energy levels. The atomic structure and the energy level of the PbV center are shown in Fig. 1(a). The centrosymmetric configuration leads to a small permanent electric dipole moment[20, 21], making it highly robust for the first-order electric field fluctuation. Thus, we can obtain stable and narrow emission over time under resonant excitation[18]. The PbV center is a spin-1/2 system with split ground and excited states. In the absence of a magnetic field, the PbV center has four possible optical transitions, in which only C and D tran-

sitions can be observed at low temperatures[14]. The C and D transitions have wavelengths of approximately 550 and 554 nm, respectively, at cryogenic temperatures (Fig. 1(b)). The energy difference between the C and D peaks corresponds to a ZFS of ~ 3900 GHz in the ground state, which is the largest among the group-IV vacancy centers in diamond. This huge ZFS effectively suppresses the phonon-mediated spin relaxation. Consequently, it is predicted the PbV center has the capability to function as a spin qubit at temperatures above the liquid helium temperature[14, 22].

The application of an external magnetic field lifts the Kramers degeneracy, thereby enabling us to access the spin degrees of freedom, generating four possible spin-related optical transitions referred to A1, A2, B1, and B2 in Fig. 1(a). The A1 and B2 transitions are spin-conserving, while the other two transitions are spin-flipping. We perform photoluminescence excitation (PLE) spectroscopy to observe the spin dependent optical transitions (Fig. 1(c)). In this measurement, we employ a cryostat equipped with a superconducting magnet to apply variable magnetic fields along the [001] direction of the diamond sample. In this configuration, the angle between the magnetic field and the quantization axis of PbV is approximately 54.7° . To prevent the PLE spectra from being invisible due to a long T_1 time [4, 5], this experiment is conducted at 13 K. At zero field, we observe a sharp resonance with a linewidth of 38 MHz derived from a single Lorentzian fitting, which corresponds to the transform-limited linewidth of the PbV center[18]. Similar to our previous work [18], the observation of the transform-limited linewidth above 10 K demonstrates the exceptional optical coherence of the PbV center benefiting from its large ZFS in the ground state. As the magnetic field strength increases, the two spin-conserving transitions become distinguishable. The split width of the spin-conserving transitions with respect to the magnetic field varies by 5.98 GHz/T. Note that although the magnetic field misalignment introduces a spin mixing[11, 23], it is thought that the mixing degree is not sufficient for the direct observation of the spin-flipping transitions.

Optically addressing the spin degrees of freedom enables us to perform time-resolved measurements to characterize the dynamic spin properties in the system. The following measurements are performed on a PbV center in solid immersion lens (SIL) to enhance the photon extraction efficiency[24]. An inset of Fig. 2(a) shows a confocal fluorescence mapping (CFM) of the target PbV in SIL, where stronger photon emission is observed from the lens with a diameter of approximately $1 \mu\text{m}$. In subsequent experiments, we utilize a neodymium magnet to apply a static magnetic field to the PbV center in another cryostat. A magnetic field with a strength of approximately 220 mT is applied along the [001] direction to the sample.

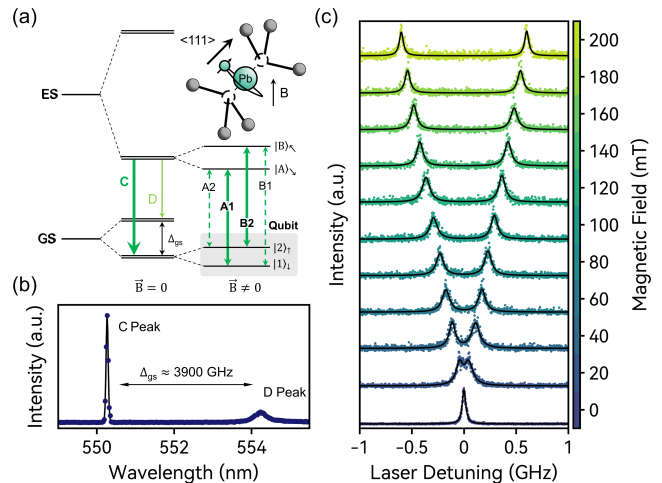


FIG. 1: Magneto-optical properties of the PbV center. (a) Atomic structure and energy level of the PbV center in diamond. (b) Cryogenic photoluminescence (PL) spectrum under non-resonant 532 nm laser excitation. (c) PLE spectra under various magnetic fields at 13 K. The color corresponds to the magnetic field strength, varied from 0 to 200 mT in 20 mT increment. The solid lines represent fits using Lorentzian functions.

We investigate the spin state initialization which occurs through the spin-flipping channel from the excited state. Following a 532 nm charge state initialization pulse with 5 ms duration[25], a resonant excitation pulse to the spin-conserving transition B2 is applied and the fluorescence in the phonon sideband (PSB) is collected. We observe a transient decay in the fluorescence intensity (Fig. 2(a)). The first non-spin-selective 532 nm laser irradiation establishes a balanced spin population in both the $|1\rangle_{\downarrow}$ and $|2\rangle_{\uparrow}$ sublevels. The following spin-selective resonant excitation pumps the population into the opposite spin state via the excited state. This process is attributed to the existence of the spin-flipping relaxation channel in the excited state, which is facilitated by the combined effects of magnetic field misalignment and Jahn-Teller effect or strain environment. Consequently, the spin state of the PbV qubit is optically initialized. The contrast between the initial fluorescence intensity and well-initialized steady state yields a spin initialization fidelity of 98.7%.

Then, we investigate the laser power dependence of the spin initialization rate (Fig. 2(b)). This dependence provides insight into the branching ratio (cyclic) η – the ratio between the spin-conserving and spin-flipping relaxation channels from the excited state. The experimental data with a saturation behavior are fitted by $\frac{\Gamma}{2} \frac{P/P_{\text{sat}}}{1+P/P_{\text{sat}}} \frac{1}{\eta}$ [26], where Γ is the spontaneous emission rate derived from the excited state lifetime. The saturation power P_{sat} and branching ratio η are fitting parameters. For the PbV center in the SIL, we extract a P_{sat} of 3.1 nW

and a branching ratio of 87. The branching ratio obtained here is comparable to that of SnV center under a similar magnetic field configuration[26].

The branching ratio is fundamentally linked to the single-shot readout (SSR) fidelity. A high branching ratio indicates that spin-conserving relaxation channel through the excited state is predominant, allowing for an extended readout time[4, 27, 28] and, consequently, a higher number of detected photons. Conversely, rapid spin-flipping relaxation channel to the opposite spin state results in poor photon detection and degrade the SSR performance. We use the sequence shown in Fig. 2(c) to evaluate SSR of the PbV center[29, 30]. To separately resonantly excite the spin-conserving A1 and B2 transitions, we use two tunable lasers that lock to the A1 and B2 transitions by PID loops from a wavemeter. Following a repump pulse of 532 nm laser irradiation, a 150 μ s pulse is applied to excite the B2 transition. This process initializes the system into the $|1\rangle_{\downarrow}$ spin state, resulting in the nearly entire electron population residing in $|1\rangle_{\downarrow}$ spin sublevel state. Following a 10 μ s time delay, a 300 μ s readout pulse resonantly excites the A1 transition, during which the continuous photon emission is accompanied by the simultaneous pumping of the electron into the opposite spin sublevel. Eventually, the population in the $|1\rangle_{\downarrow}$ sublevel is almost depleted. After 10 μ s idle time, a resonant pulse (referred to dark pulse) to the A1 transition is applied again. Due to the absence of the electron population in this sublevel, only few photons could be detected. We repeat this sequence 10,000 times, recording the photon number detected in each readout and dark pulse. The photon number statistics are shown in Fig. 2(d). Benefiting from the enhanced photon extraction efficiency with the SIL structure, we detect 4.83 photons on average for the readout pulse. In contrast, the average count during the dark pulses is 0.64. We set one photon as a discrimination threshold between the bright and dark states. The SSR fidelity is defined as $\mathcal{F}_{SSR} = 1 - \mathcal{E}$ [31], where $\mathcal{E} = \frac{1}{2}(\mathcal{E}_R + \mathcal{E}_D)$. The \mathcal{E}_R (\mathcal{E}_D) is the possibility of obtaining photon counts below (above) the threshold during a single readout (dark) pulse. We achieve a SSR fidelity of 76%, which is comparable to those of the GeV[27] and SnV[29] under the similar magnetic field configuration. This value surpasses the 50% threshold of random guessing, demonstrating the feasibility of SSR for the PbV center even placed in a large off-axis magnetic field environment.

On the basis of the spin state initialization and readout above, we evaluate longitudinal spin relaxation time (T_1) of the PbV center. The upper panel in Fig. 3(a) depicts the measurement sequence. After the charge state stabilization pulse, the initial spin-selective B2 excitation polarizes the electron population into the $|1\rangle_{\downarrow}$ spin sublevel. A varied time delay is introduced to allow the phonon-mediated relaxation. Finally, a B2 pulse is applied to probe the recovered population into the $|2\rangle_{\uparrow}$

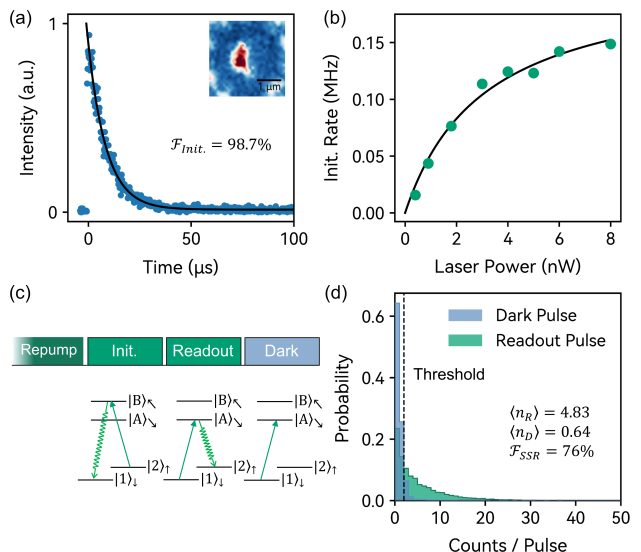


FIG. 2: Spin initialization and SSR performance of the PbV center at 7.5 K (a) Spin initialization. Inset shows a CFM image of the PbV in SIL. (b) Spin initialization rate as a function of the resonant laser power. Solid line denotes the fitting described in the main text. (c) Pulse sequence implemented for the SSR measurement. (d) Photon counting statistics derived from the sequence in (c). The threshold is set to one photon per pulse to discriminate the bright and dark states, yielding a SSR fidelity of 76%.

state, thereby quantifying the spin-flip probability induced by the phonon interaction during the delay time. Here, photons in a 10 μ s collection window are extracted for data analysis. As shown in Fig. 3(a), the fluorescence counts gradually recover toward saturation as the delay time increases, indicating the relaxation of the spin population back to the thermal equilibrium via the electron-phonon interaction. We fit the result with a mono-exponential function, resulting in $T_1 = 12(2)$ ms at 7.5 K, which is the highest value under similar magnetic field configuration at this temperature in the group-IV vacancy centers in diamond[32–36]. For T_1 over 10 ms under similar magnetic field configuration, the SnV center should be below the liquid helium temperature regime [36]. This fact confirms that the electron-phonon interaction is largely suppressed by the large ZFS in the ground state for the PbV center.

Figure 3(b) shows the temperature dependence of T_1 . As a function of inverse temperature on a semi-logarithmic scale. We first attempt to describe the temperature dependence of T_1 using a modified Orbach process defined by the function $\frac{1}{T_1} \propto \frac{\Delta_{gs}^3}{\exp\left(\frac{\alpha h \Delta_{gs}}{k_B T}\right) - 1}$ [37], where Δ_{gs} is a ground state splitting of 3903 GHz for the emitter used here and α is a scaling factor. The fitting to this function, shown as a dashed line in Fig. 3(b), yields

a scaling factor of 0.5. However, the Orbach process[38] is a fundamentally resonant two-phonon process that requires a real additional energy level, which is the upper branch level for the group-IV vacancy centers. Thus, the obtained scaling factor of 0.5 is inconsistent with this physical model. A possible explanation is the additional contribution from the Raman process. A model incorporating a Raman term ($1/T_1 \propto T^7$)[39] with the Orbach process with $\alpha=1$ fits the results well (solid line in Fig. 3(b)). Therefore, we suggest that the spin-lattice relaxation of PbV at this temperature regime is governed adjointly by the Orbach and Raman processes.

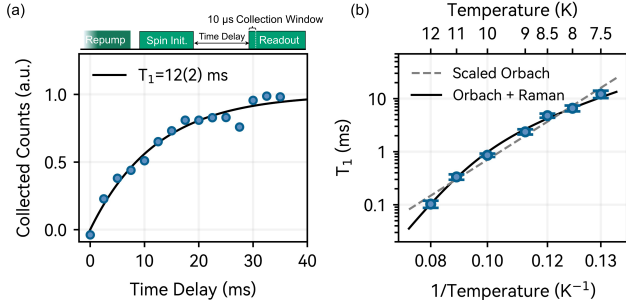


FIG. 3: Longitudinal relaxation time. (a) T_1 measurement at 7.5 K. (b) Temperature dependence of T_1 .

Finally, we observe the coherent dark state of the PbV spin via coherent population trapping (CPT). CPT is an all-optical method to probe the phase coherence of a spin system by using a shared excited state[32, 40]. As shown in an inset of Fig. 4(a), a pump laser is locked to a spin-conserving transition of B2, while a second probe laser is scanned in the frequency domain relative to the pump laser. The frequency offset between the two lasers is defined as the Raman frequency. When the probe laser satisfies the zero two-photon detuning condition, i.e., becoming resonant to the shared excited state, a Λ scheme is established. In this scheme, destructive quantum interference traps the electron population in a non-interacting superposition dark state, resulting in the observation of a dip in spectrum. Here, we implement a phase modulation electro-optic modulator to realize high mutual optical coherence of the pump and probe lasers during the Raman frequency scanning. The sequence used for CPT is shown at the upper panel of Fig. 4(a). Following charge state stabilization pulse, the electron population is initialized to $|1\rangle_{\downarrow}$. Then, the pump and probe lasers are simultaneously irradiated to the PbV center. This sequence is repeated for different Raman frequencies. In a representative CPT curve in Fig. 4(a), a high-contrast fluorescence dip is clearly observed, signifying the formation of a coherent dark state. A black solid line is the model fit based on the Lindblad master equation[41]. The frequency of the resonance dip corresponds to a qubit frequency of 4.24 GHz between the sublevels $|1\rangle_{\downarrow}$ and $|2\rangle_{\uparrow}$. The intrinsic linewidth of a CPT dip is fundamentally determined

by the spin dephasing time (T_2^*). To eliminate the effect of power broadening, we perform a power dependent measurement and extract the linewidths of the CPT dip by Lorentzian function fitting. Figure 4(b) shows that the CPT linewidth measured at 6.5 K becomes narrower as the laser power is reduced. We summarize the CPT linewidth as a function of the laser power in Fig. 4(c). At the minimum power limit, we observe the narrowest linewidth of 0.9(6) MHz, corresponding to a spin dephasing time of 354 ns. This value is in agreement with the T_2^* of other group-IV vacancy centers typically observed in natural abundance diamond samples[4, 36, 37, 42]. Thus, the decoherence is thought to be primarily governed by the spin bath noise, rather than phonon-mediated decoherence even at a temperature above 4 K.

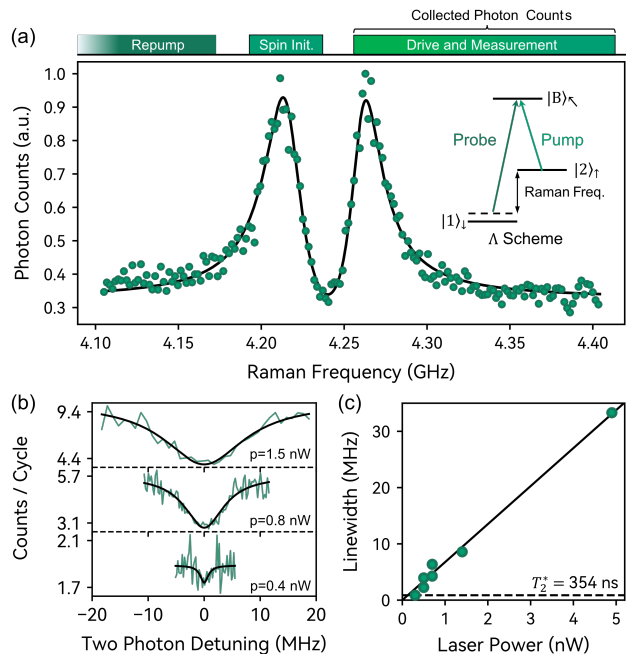


FIG. 4: CPT of the PbV center. (a) Sequence and a representative CPT spectrum at 7 K. The black solid line represents a numerical fit based on the Lindblad master equation. (b) Evolution of the CPT spectra as varying the laser power at 6.5 K. (c) CPT linewidth as a function of the total incident laser power at 6.5 K. The narrowest observed linewidth is 0.9(6) MHz, corresponding to a spin dephasing time (T_2^*) of 354 ns.

The evaluation of T_1 underscored the extraordinary potential of the PbV center for the operation above the liquid helium temperature. Under a significant off-axis magnetic field, we recorded T_1 of 12 ms at 7.5 K. This performance significantly shifts the temperature benchmark for achieving $T_1 > 10$ ms compared to the 3.25 K reported for the SnV center[36] under similar magnetic field condition. Also, at 6.5 K, the spin dephasing time has reached the spin-bath limitation[4, 36, 37, 42], indicating

that phonon-mediated decoherence is not the bottleneck for the decoherence. A ^{12}C enriched diamond could further mitigate the spin bath noise[4–6, 43], thereby significantly reducing the phase noise and extending the spin dephasing time. Such an isotopically purified environment also creates a favorable condition for achieving a long spin coherence time. According to the prior study on SnV[6], the T_1 of PbV centers can be enhanced by several orders of magnitude through precise magnetic field alignment to the symmetry axis, suggesting that T_1 potentially exceeds 1 s at temperature well above 4 K. Therefore, we have a reasonable expectation that at elevated temperature, the PbV center can achieve a long spin coherence time that are comparable to those of SiV and GeV at dilution refrigerator temperatures and SnV centers at temperature around 2 K.

In this work, we report the spin properties of the PbV center in diamond using all-optical methods. We demonstrated the feasibility of SSR, long spin lifetimes, and spin-bath-limited spin dephasing time of the PbV center above 4 K. The excellent thermal robustness of PbV over 4 K not only allows for significantly relaxed cryogenic equipment but also enables the use of a higher microwave power for the faster gate operation under the microwave spin control scheme in the future, which makes the PbV center as an attractive candidate for nodes in scalable quantum networks.

The authors would like to thank Ryotaro Abe and Keita Ikeda for experimental support. We thank Materials Analysis Division, Core Facility Center, Institute of Science Tokyo for technical assistance. This work is supported by JSPS KAKENHI Grant Number 25K24501, the MEXT Quantum Leap Flagship Program (MEXT Q-LEAP) Grant Number JPMXS0118067395, JST Moonshot R&D Grant Number JPMJMS2062, JST ASPIRE JPMJAP24C1, JST SPRING Grant Number JPMJSP2180, and Council for Science, Technology and Innovation (CSTI), 3rd Cross-ministerial Strategic Innovation Promotion Program (SIP) Quantum.

* Corresponding author: iwasaki.t.c5b4@m.isct.ac.jp

- [1] H. J. Kimble, The quantum internet, *Nature* **453**, 1023 (2008).
- [2] D. D. Awschalom, R. Hanson, J. Wrachtrup, and B. B. Zhou, Quantum technologies with optically interfaced solid-state spins, *Nature Photonics* **12**, 516 (2018).
- [3] T. Yamamoto, H. B. van Ommen, K.-N. Schymik, B. de Zoeten, S. Onoda, S. Saiki, T. Ohshima, H. Arjmandi-Tash, R. Vollmer, and T. H. Taminiau, Tens-second electron-spin coherence in isotopically engineered diamond (2026), arXiv:2604.07439.
- [4] D. Sukachev, A. Sipahigil, C. Nguyen, M. Bhaskar, R. Evans, F. Jelezko, and M. Lukin, Silicon-vacancy spin qubit in diamond: A quantum memory exceeding 10 ms with single-shot state readout, *Phys. Rev. Lett.* **119**, 223602 (2017).
- [5] K. Senkalla, G. Genov, M. H. Metsch, P. Siyushev, and F. Jelezko, Germanium vacancy in diamond quantum memory exceeding 20 ms, *Phys. Rev. Lett.* **132**, 026901 (2024).
- [6] X. Guo, A. M. Stramma, Z. Li, W. G. Roth, B. Huang, Y. Jin, R. A. Parker, J. A. Martínez, N. Shofer, C. P. Michaels, C. P. Purser, M. H. Appel, E. M. Alexeev, T. Liu, A. C. Ferrari, D. D. Awschalom, N. Delegan, B. Pingault, G. Galli, F. J. Heremans, M. Atatüre, and A. A. High, Microwave-based quantum control and coherence protection of tin-vacancy spin qubits in a strain-tuned diamond-membrane heterostructure, *Phys. Rev. X* **13**, 041037 (2023).
- [7] I. Karapatzakis, J. Resch, M. Schrodin, P. Fuchs, M. Kischneck, J. Heupel, L. Kussi, C. Sürgers, C. Popov, J. Meijer, C. Becher, W. Wernsdorfer, and D. Hunger, Microwave control of the tin-vacancy spin qubit in diamond with a superconducting waveguide, *Phys. Rev. X* **14**, 031036 (2024).
- [8] R. E. Evans, M. K. Bhaskar, D. D. Sukachev, C. T. Nguyen, A. Sipahigil, M. J. Burek, B. Machielse, G. H. Zhang, A. S. Zibrov, E. Bielejec, H. Park, M. Lončar, and M. D. Lukin, Photon-mediated interactions between quantum emitters in a diamond nanocavity, *Science* **362**, 662 (2018).
- [9] N. Codreanu, T. Turan, D. B. Rodriguez, M. Pasini, L. de Santis, M. Ruf, C. F. Primavera, L. G. C. Wienhoven, C. E. Smulders, S. Gröblacher, and R. Hanson, Above-unity coherent cooperativity of tin-vacancy centers in diamond photonic crystal cavities (2025), arXiv:2511.13375.
- [10] M. Pompili, S. L. N. Hermans, S. Baier, H. K. C. Beukers, P. C. Humphreys, R. N. Schouten, R. F. L. Vermeulen, M. J. Tiggelman, L. dos Santos Martins, B. Dirkse, S. Wehner, and R. Hanson, Realization of a multinode quantum network of remote solid-state qubits, *Science* **372**, 259 (2021).
- [11] C. Hepp, T. Müller, V. Waselowski, J. N. Becker, B. Pingault, H. Sternschulte, D. Steinmüller-Nethl, A. Gali, J. R. Maze, M. Atatüre, and C. Becher, Electronic structure of the silicon vacancy color center in diamond, *Phys. Rev. Lett.* **112**, 036405 (2014).
- [12] T. Iwasaki, F. Ishibashi, Y. Miyamoto, Y. Doi, S. Kobayashi, T. Miyazaki, K. Tahara, K. D. Jahnke, L. J. Rogers, B. Naydenov, F. Jelezko, S. Yamasaki, S. Nagamachi, T. Inubushi, N. Mizuochi, and M. Hatano, Germanium-vacancy single color centers in diamond, *Scientific Reports* **5**, 12882 (2015).
- [13] T. Iwasaki, Y. Miyamoto, T. Taniguchi, P. Siyushev, M. H. Metsch, F. Jelezko, and M. Hatano, Tin-vacancy quantum emitters in diamond, *Phys. Rev. Lett.* **119**, 253601 (2017).
- [14] P. Wang, T. Taniguchi, Y. Miyamoto, M. Hatano, and T. Iwasaki, Low-temperature spectroscopic investigation of lead-vacancy centers in diamond fabricated by high-pressure and high-temperature treatment, *ACS Photonics* **8**, 2947 (2021).
- [15] C. M. Knaut, A. Suleymanzade, Y.-C. Wei, D. R. Assumpcao, P.-J. Stas, Y. Q. Huan, B. Machielse, E. N. Knall, M. Sutula, G. Baranes, N. Sinclair, C. De-Eknamkul, D. S. Levonian, M. K. Bhaskar, H. Park, M. Lončar, and M. D. Lukin, Entanglement of nanopho-

- tonic quantum memory nodes in a telecom network, *Nature* **629**, 573 (2024).
- [16] Y.-C. Wei, P.-J. Stas, A. Suleymanzade, G. Baranes, F. Machado, Y. Q. Huan, C. M. Knaut, S. W. Ding, M. Merz, E. N. Knall, U. Yazlar, M. Sirotin, I. W. Wang, B. Machielse, S. F. Yelin, J. Borregaard, H. Park, M. Lončar, and M. D. Lukin, Universal distributed blind quantum computing with solid-state qubits, *Science* **388**, 509 (2025).
- [17] P.-J. Stas, Y.-C. Wei, M. Sirotin, Y. Q. Huan, U. Yazlar, F. A. Arias, E. Knyazev, G. Baranes, B. Machielse, S. Grandi, D. Riedel, J. Borregaard, H. Park, M. Lončar, A. Suleymanzade, and M. D. Lukin, Entanglement-assisted non-local optical interferometry in a quantum network, *Nature* **651**, 326 (2026).
- [18] P. Wang, L. Kazak, K. Senkalla, P. Siyushev, R. Abe, T. Taniguchi, S. Onoda, H. Kato, T. Makino, M. Hatano, F. Jelezko, and T. Iwasaki, Transform-limited photon emission from a lead-vacancy center in diamond above 10 K, *Phys. Rev. Lett.* **132**, 073601 (2024).
- [19] R. Abe, Y. Chen, P. Wang, T. Taniguchi, M. Miyakawa, S. Onoda, M. Hatano, and T. Iwasaki, Narrow inhomogeneous distribution and charge state stabilization of lead-vacancy centers in diamond, *Adv. Funct. Mater.* **36**, e12412 (2026).
- [20] L. D. Santis, M. E. Trusheim, K. C. Chen, and D. R. Englund, Investigation of the stark effect on a centrosymmetric quantum emitter in diamond, *Phys. Rev. Lett.* **127**, 147402 (2021).
- [21] S. Aghaeimeibodi, D. Riedel, A. E. Rugar, C. Dory, and J. Vučković, Electrical tuning of tin-vacancy centers in diamond, *Phys. Rev. Appl.* **15**, 064010 (2021).
- [22] M. Ruf, N. H. Wan, H. Choi, D. Englund, and R. Hanson, Quantum networks based on color centers in diamond, *J. Appl. Phys.* **130**, 070901 (2021).
- [23] G. Thiering and A. Gali, *Ab Initio* magneto-optical spectrum of Group-IV vacancy color centers in Diamond, *Phys. Rev. X* **8**, 021063 (2018).
- [24] K. Hirai, E. Ota, Y. Chen, R. Kato, P. Wang, T. Makino, T. Taniguchi, M. Miyakawa, S. Onoda, M. Hatano, and T. Iwasaki, in preparation.
- [25] Y. Chen, Y. Miyamoto, E. Ota, R. Abe, T. Taniguchi, S. Onoda, M. Hatano, and T. Iwasaki, Optical charge state manipulation of lead-vacancy centers in diamond, *Nano Lett.* **25**, 16697 (2025).
- [26] R. Debroux, C. P. Michaels, C. M. Purser, N. Wan, M. E. Trusheim, J. A. Martínez, R. A. Parker, A. M. Stramma, K. C. Chen, L. de Santis, E. M. Alexeev, A. C. Ferrari, D. Englund, D. A. Gangloff, and M. Atatüre, Quantum control of the tin-vacancy spin qubit in diamond, *Phys. Rev. X* **11**, 041041 (2021).
- [27] D. Chen, J. E. Fröch, S. Ru, H. Cai, N. Wang, G. Adamo, J. Scott, F. Li, N. Zheludev, I. Aharonovich, and W. Gao, Quantum interference of resonance fluorescence from germanium-vacancy color centers in diamond, *Nano Lett.* **22**, 6306 (2022).
- [28] E. I. Rosenthal, S. Biswas, G. Scuri, H. Lee, A. J. Stein, H. C. Kleidermacher, J. Grzesik, A. E. Rugar, S. Aghaeimeibodi, D. Riedel, M. Titze, E. S. Bielejec, J. Choi, C. P. Anderson, and J. Vučković, Single-shot readout and weak measurement of a tin-vacancy qubit in diamond, *Phys. Rev. X* **14**, 041008 (2024).
- [29] J. Görlitz, D. Herrmann, P. Fuchs, T. Iwasaki, T. Taniguchi, D. Rogalla, D. Hardeman, P. O. Colard, M. Markham, M. Hatano, and C. Becher, Coherence of a charge stabilised tin-vacancy spin in diamond, *npj Quantum Inf.* **8**, 45 (2022).
- [30] P. Gundlapalli, P. J. Vetter, G. Genov, M. Olney-Fraser, P. Wang, M. M. Müller, K. Senkalla, and F. Jelezko, High-fidelity single-shot readout and selective nuclear spin control for a spin-1/2 quantum register in diamond (2025), arXiv:2510.09164.
- [31] A. H. Myerson, D. J. Szwer, S. C. Webster, D. T. C. Allcock, M. J. Curtis, G. Imreh, J. A. Sherman, D. N. Stacey, A. M. Steane, and D. M. Lucas, High-fidelity readout of trapped-ion qubits, *Phys. Rev. Lett.* **100**, 200502 (2008).
- [32] L. J. Rogers, K. D. Jahnke, M. H. Metsch, A. Sipahigil, J. M. Binder, T. Teraji, H. Sumiya, J. Isoya, M. D. Lukin, P. Hemmer, and F. Jelezko, All-optical initialization, readout, and coherent preparation of single silicon-vacancy spins in diamond, *Phys. Rev. Lett.* **113**, 263602 (2014).
- [33] J. N. Becker, B. Pingault, D. Groß, M. Gündoğan, N. Kukharchyk, M. Markham, A. Edmonds, M. Atatüre, P. Bushev, and C. Becher, All-optical control of the silicon-vacancy spin in diamond at millikelvin temperatures, *Phys. Rev. Lett.* **120**, 053603 (2018).
- [34] B. Pingault, D.-D. Jarausch, C. Hepp, L. Klintberg, J. N. Becker, M. Markham, C. Becher, and M. Atatüre, Coherent control of the silicon-vacancy spin in diamond, *Nat. Commun.* **8**, 15579 (2017).
- [35] P. Siyushev, M. H. Metsch, A. Ijaz, J. M. Binder, M. K. Bhaskar, D. D. Sukachev, A. Sipahigil, R. E. Evans, C. T. Nguyen, M. D. Lukin, P. R. Hemmer, Y. N. Palyanov, I. N. Kupriyanov, Y. M. Borzdov, L. J. Rogers, and F. Jelezko, Optical and microwave control of germanium-vacancy center spins in diamond, *Phys. Rev. B* **96**, 081201 (2017).
- [36] M. E. Trusheim, B. Pingault, N. H. Wan, M. Gündoğan, L. D. Santis, R. Debroux, D. Gangloff, C. Purser, K. C. Chen, M. Walsh, J. J. Rose, J. N. Becker, B. Lienhard, E. Bersin, I. Paradeisanos, G. Wang, D. Lyzwa, A. R.-P. Montblanch, G. Malladi, H. Bakhru, A. C. Ferrari, I. A. Walmsley, M. Atatüre, and D. Englund, Transform-limited photons from a coherent tin-vacancy spin in diamond, *Phys. Rev. Lett.* **124**, 023602 (2020).
- [37] E. I. Rosenthal, C. P. Anderson, H. C. Kleidermacher, A. J. Stein, H. Lee, J. Grzesik, G. Scuri, A. E. Rugar, D. Riedel, S. Aghaeimeibodi, G. H. Ahn, K. V. Gasse, and J. Vučković, Microwave spin control of a tin-vacancy qubit in diamond, *Phys. Rev. X* **13**, 031022 (2023).
- [38] K. D. Jahnke, A. Sipahigil, J. M. Binder, M. W. Doherty, M. Metsch, L. J. Rogers, N. B. Manson, M. D. Lukin, and F. Jelezko, Electron-phonon processes of the silicon-vacancy centre in diamond, *New J. Phys.* **17**, 043011 (2015).
- [39] G. Wolfowicz, F. J. Heremans, C. P. Anderson, S. Kanai, H. Seo, A. Gali, G. Galli, and D. D. Awschalom, Quantum guidelines for solid-state spin defects, *Nat. Rev. Mater.* **6**, 906 (2021).
- [40] B. Pingault, J. N. Becker, C. H. Schulte, C. Arend, C. Hepp, T. Godde, A. I. Tartakovskii, M. Markham, C. Becher, and M. Atatüre, All-optical formation of coherent dark states of silicon-vacancy spins in diamond, *Phys. Rev. Lett.* **113**, 263601 (2014).
- [41] G. Lindblad, On the generators of quantum dynamical semigroups, *Commun. Math. Phys.* **48**, 119 (1976).

- [42] Y.-I. Sohn, S. Meesala, B. Pingault, H. A. Atikian, J. Holzgrafe, M. Gündoğan, C. Stavrakas, M. J. Stanley, A. Sipahigil, J. Choi, M. Zhang, J. L. Pacheco, J. Abraham, E. Bielejec, M. D. Lukin, M. Atatüre, and M. Lončar, Controlling the coherence of a diamond spin qubit through its strain environment, *Nat. Commun.* **9**, 2012 (2018).
- [43] G. Balasubramanian, P. Neumann, D. Twitchen, M. Markham, R. Kolesov, N. Mizuochi, J. Isoya, J. Achard, J. Beck, J. Tessler, V. Jacques, P. R. Hemmer, F. Jelezko, and J. Wrachtrup, Ultralong spin coherence time in isotopically engineered diamond, *Nat. Mater.* **8**, 383 (2009).